ISSN 1063-7834, Physics of the Solid State, 2018, Vol. 60, No. 7, pp. 1413–1418. © Pleiades Publishing, Ltd., 2018.
Original Russian Text © R.R. Altunin, E.T. Moiseenko, S.M. Zharkov, 2018, published in Fizika Tverdogo Tela, 2018, Vol. 60, No. 7, pp. 1397–1402.

Structural Phase Transformations in Al/Pt Bilayer Thin Films during the Solid-State Reaction

R. R. Altunin[a, *], **E. T. Moiseenko**[a], **and S. M. Zharkov**[b, a]
[a] *Siberian Federal University, Krasnoyarsk, 660041 Russia*
[b] *Kirensky Institute of Physics, Krasnoyarsk Scientific Center, Siberian Branch, Russian Academy of Sciences, Krasnoyarsk, 660036 Russia*
**e-mail: raltunin@gmail.com*

Received December 20, 2017

Abstract—A sequence of phases forming during the solid-phase reaction in Al/Pt bilayer thin films has been investigated by in situ electron diffraction. It is shown that the amorphous $PtAl_2$ phase forms first during the solid-phase reaction initiated by heating. Upon further heating, $PtAl_2$, Pt_2Al_3, PtAl, and Pt_3Al crystalline phases sequentially form, which is qualitatively consistent with an effective formation heat model. The content of phases forming during the reaction has been quantitatively analyzed and the structural phase transformations have been examined.

DOI: 10.1134/S106378341807003X

1. INTRODUCTION

Aluminum-containing compounds find wide application in microelectronic production as electric contacts, metallizing layers, and diffusion barriers and are used to increase the stability of systems against electric migration [1–3]. Al–Pt intermetallic compounds with the shape memory effect [6] are used in microelectronic devices [4, 5], as refractory alloys [7, 8], and in designing solar cells [9].

The reliability of microelectronic devices is determined by the stability of the physicochemical properties of thin-film systems included in electronic components. In view of this, it is important to study the solid-state reactions occurring at the interface between nanolayers with different compositions. The solid-state reaction results in the formation of new compounds with the physicochemical properties different from those of an original thin-film system. For example, heating of an Al/Pt thin-film bilayer used in ferroelectric random access memory (FeRAM) [10, 11] to 200–300°C leads to the failure of these devices because of formation of intermetallic compounds at the interface between the aluminum and platinum layers.

It is worth noting that the experimentally observed phase sequence at the solid-state reaction in Al/Pt thin films is described by none of the available theoretical models. The theoretical calculations in the framework of effective heat formation (EHF) [12] and Walser–Bene [13] models showed that the Pt_5Al_{21} phase should form first during the solid-state reaction. However, in experimental studies [14, 15], the formation of the $PtAl_2$ amorphous phase was observed first and, in [16–19], it was the Pt_2Al_3 crystalline phase. According to the literature data, most of the investigated solid-state reactions in Al/Pt films occur at the initial stage. There are few works, e.g., [18, 20], on studying a total phase sequence. This is, probably, due to the fact that during the solid-state reactions in an Al–Pt system, a great number of intermetallic compounds form that are difficult to identify [18]. It should be noted that most of the studies on the solid-state reactions in the Al/Pt thin-film systems were carried out after long-term annealing at a fixed temperature. In this case, the phase composition is only investigated at certain stages of the experiment, which does not allow the exact sequence of phases forming during the solid-state reaction to be determined. In addition, it is interesting that in thin films with thicknesses of no more than 100 nm, in contrast to the films with thicknesses of no less than 100 nm, not all the phases reflected in the equilibrium phase diagram are formed [12].

The aim of this study was to establish a sequence of phases forming during the solid-state reaction in Al/Pt bilayer thin films. The investigations were carried out by in situ electron diffraction, which allowed us to examine the phase composition variation directly during the solid-state reaction.

2. EXPERIMENTAL

The Al/Pt bilayer thin films under study were obtained by electron beam evaporation on a

MED-020 high-vacuum facility (Bal-Tec). Sputtering was performed in vacuum at a residual pressure of 5×10^{-5} Pa. Film thickness was controlled using a QSG-100 quartz resonator, which allows controlling the integrated film thickness accurate to 0.01 nm. The individual aluminum and platinum layer thicknesses were chosen to obtain an Al : Pt atomic ratio of 1 : 1. Freshly cleaved NaCl single crystals and cover glass were used as substrates. In deposition, ADVENT high-purity Pt (99.99%) and Al (99.999%) materials were used [21]. For the electron microscopy investigations, the films formed on NaCl were separated from the substrate in distilled water and deposited onto supporting molybdenum electron-microscopy grids.

The microstructure and elemental composition of the thin films were examined on a JEOL JEM-2100 transmission electron microscope (the accelerating voltage is 200 kV) equipped with an Oxford Inca x-sight energy dispersive spectrometer. The phase composition of the investigated samples was determined from electron diffraction patterns obtained by microdiffraction from areas ~0.1–1.0 μm in diameter. Heating was performed directly in the JEM-2100 transmission electron microscope column (the base vacuum corresponded to 1×10^{-6} Pa) using a special Gatan Model 652 double tilt heating holder for controlling sample heating from room temperature to +1000°C. This method was successfully used to study the solid-state reactions in Fe/Pd [22, 23] and Fe/Si [24] thin-film systems.

The obtained electron diffraction patterns were analyzed using the Process Diffraction program [25] to determine the quantitative content of the phases forming during the solid-state reaction. As was shown in [25], the relative error in determining the content of a single phase using this software is ±10%. The absolute intensities of diffraction reflections were theoretically calculated using the Endeavour software [26].

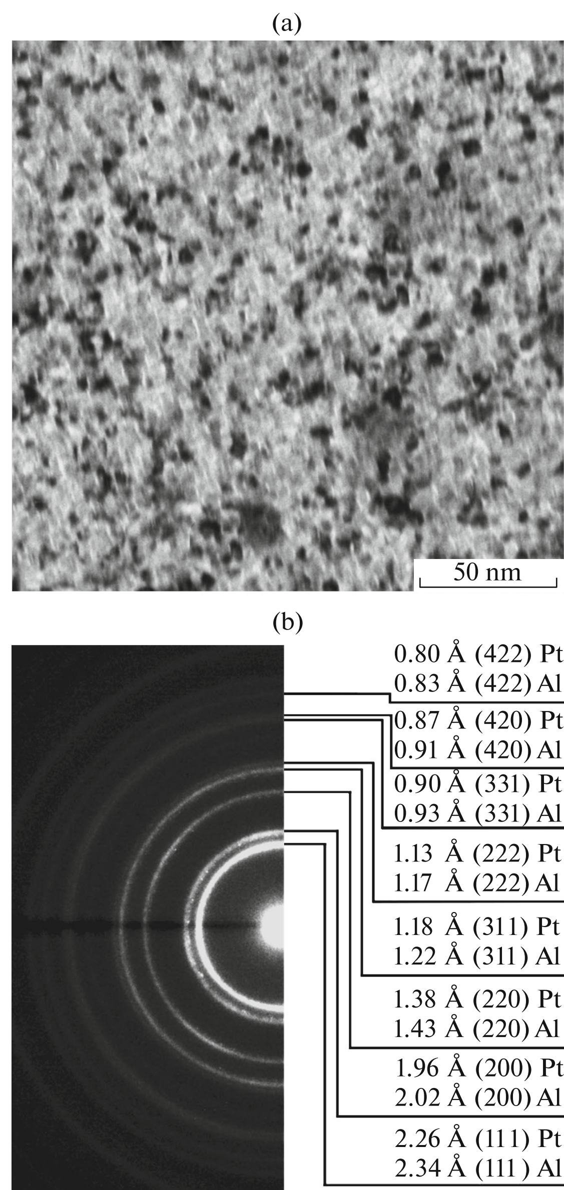

Fig. 1. (a) Electron microscopy image and (b) electron diffraction pattern of the initial Al/Pt film.

3. RESULTS

A series of Al/Pt bilayer thin films with a total thickness of up to 50 nm was obtained. Electron microscopy studies of the initial Al/Pt films revealed platinum and aluminum crystallite sizes of 4–6 and 5–20 nm, respectively (Fig. 1a). The electron diffraction pattern (Fig. 1b) obtained from the initial film contains diffraction reflections belonging to the face-centered cubic (fcc) phases: A1 (sp. gr. $Fm\overline{3}m$, the lattice parameter is $a = 4.05$ Å) and Pt (sp. gr. $Fm\overline{3}m$, the lattice parameter is $a = 3.91$ Å).

In order to obtain information on the phase formation during the solid-state reaction, the Al/Pt films were subjected to a series of heatings from room temperature to 500°C at a rate of 10°C/min. Simultaneously with the sample heating, electron diffraction patterns were recorded at a rate of four frames per minute; i.e., one frame corresponded to the sample temperature variation by 2.5°C. Analysis of the electron diffraction patterns allowed us to study the change in the phase composition of the films. The data on the phases formed in the films during the solid-state reaction is given in Table 1.

The beginning of the solid-state reaction between the aluminum and platinum nanolayers was detected at a temperature of ~270°C, which was accompanied by the occurrence of low-intensity diffuse halos in the electron diffraction patterns. The observed halos correspond to interplanar distances of ≈3.4, ≈2.9, and ≈2.1 Å, which can be attributed to the diffraction reflections $d(111)$ = 3.41 Å, $d(200)$ = 2.95 Å, and

Table 1. Structural phase transformations during the solid-state reaction in the Al/Pt bilayer thin films

Phase	Temperature, °C								
	25–269	270–287	288–300	301–349	350–389	390–429	430–459	460–497	498–500
Al	+	+	+						
Pt	+	+	+	+	+	+			
$PtAl_2$ (amorphous)		+	+						
$PtAl_2$			s	s	s	s	s		
Pt_2Al_3			+	+	+	+	+	+	s
PtAl					+	+	+	+	+
Pt_5Al_3						?			
Pt_2Al						?			
Pt_3Al						s	+	+	s

Symbol s indicates that the phase content in a film is small (<10 wt %). Question mark denotes that the presence of a phase is not excluded.

$d(220) = 2.09$ Å of the $PtAl_2$ phase (sp. gr. $Fm\bar{3}m$, the lattice parameter is $a = 5.91$ Å). This is consistent with the results reported in [14, 15], where the solid-state reaction in the Al/Pt films was shown to begin with the formation of an amorphous phase with the elemental composition similar to $PtAl_2$.

At a temperature of 288°C, the low-intensity diffraction reflections corresponding to the $PtAl_2$ crystalline phase were observed in the electron diffraction pattern: $d(111) = 3.41$ Å, $d(220) = 2.09$ Å, and $d(311) = 1.78$ Å. This is indicative of the beginning of the transition of this phase from amorphous to crystalline. At $T = 291$°C, the occurrence of diffraction reflections of the Pt_2Al_3 phase (sp. gr. $P\bar{3}m1$, the lattice parameters are $a = 4.21$ Å and $c = 5.17$ Å) was observed: $d(001) = 5.17$ Å, $d(101) = 2.98$ Å, and $d(012) = 2.11$ Å. At a temperature of 350°C, the occurrence of reflections of the PtAl phase (sp. gr. $Pm\bar{3}m$, the lattice parameter is $a = 3.04$ Å) was observed and at 390°C, the reflections of the Pt_3Al phase (sp. gr. $Pm\bar{3}m$, $a = 3.87$ Å) were detected.

Electron microscopy study of the Al/Pt thin films after heating to 500°C showed that they consist of crystallites with an average size of 15–25 nm (Fig. 2a). The electron diffraction pattern (Fig. 2b) obtained after heating the film to 500°C contains diffraction reflections of the PtAl, Pt_2Al_3, and Pt_3Al phases. The total Pt_2Al_3 and Pt_3Al phase content is lower than 10 wt %.

In order to study the structural-phase transformations, the content of the phases formed during the solid-state reaction was quantitatively analyzed. It should be noted that the quantitative estimation of the fcc aluminum phase content by analyzing the diffraction reflection intensities in the electron diffraction patterns is complicated because the fcc aluminum and platinum crystal lattice parameters differ by only 3.5%; i.e., the corresponding diffraction reflections are close to each other. The absolute intensity of the fcc aluminum diffraction reflections is lower than the intensity of analogous reflections for platinum by almost an order of magnitude ($I_{abs}(111) = 509$ for Al and $I_{abs}(111) = 4856$ for Pt). In view of the aforesaid, it is impossible to quantitatively estimate the aluminum fcc phase content in the presence of fcc platinum. Therefore, as long as the sample contains the fcc aluminum phase (~300°C), we cannot quantitatively analyze the contents of forming phases.

The quantitative analysis of the contents of phases formed during the solid-state reaction was performed in the temperature range from 310 to 500°C. Figure 3 shows the phase composition variation during the solid-state reaction in the Al/Pt films; the contents of individual phases are given in weight percent. It is noteworthy that the quantitative analysis can only be performed when the intensities of diffraction reflections of the forming phases become sufficient high. In the PtAl phase, the absolute intensity of the diffraction reflection with the maximum intensity is $I_{abs}(110) = 709$, which is much lower than the absolute intensity of the reflections of Pt ($I_{abs}(111) = 4856$), $PtAl_2$ ($I_{abs}(220) = 16148$), and Pt_2Al_3 ($I_{abs}(110) = 1682$), which also have the maximum intensity for these phases. In this case, the diffraction reflections of the PtAl, fcc platinum, Pt_2Al_3, and $PtAl_2$ phases, which have the maximum intensity, are close to each other in the electron diffraction pattern. Therefore, we cannot determine the exact temperature of the onset of PtAl phase formation and the content of this phase can only be analyzed after attaining a temperature of 350°C (Fig. 3), when the PtAl phase content is ~20 wt %.

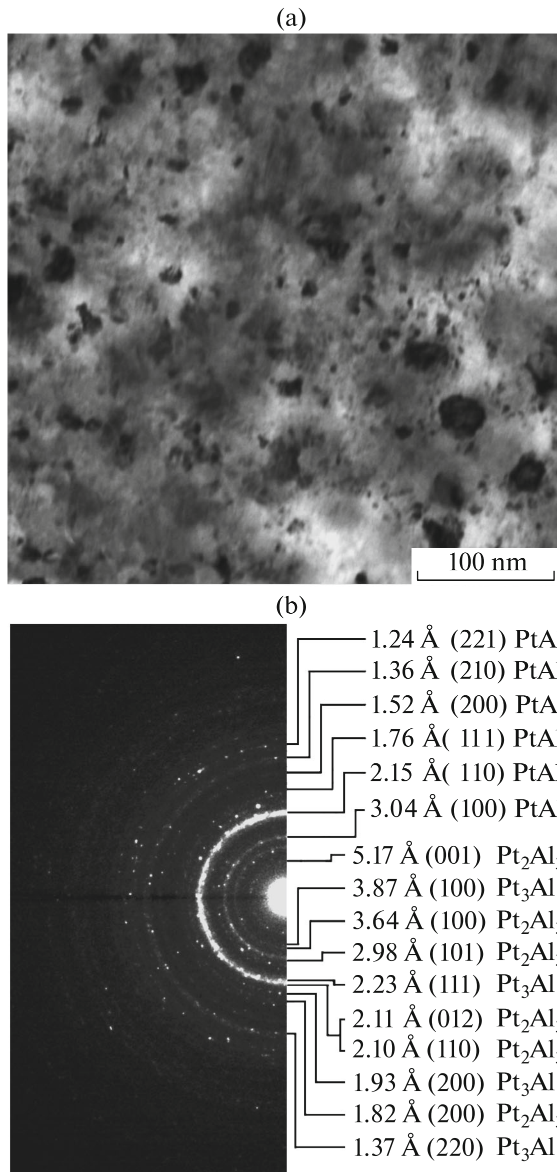

Fig. 2. (a) Electron microscopy image and (b) electron diffraction pattern of the Al/Pt film after heating to 500°C.

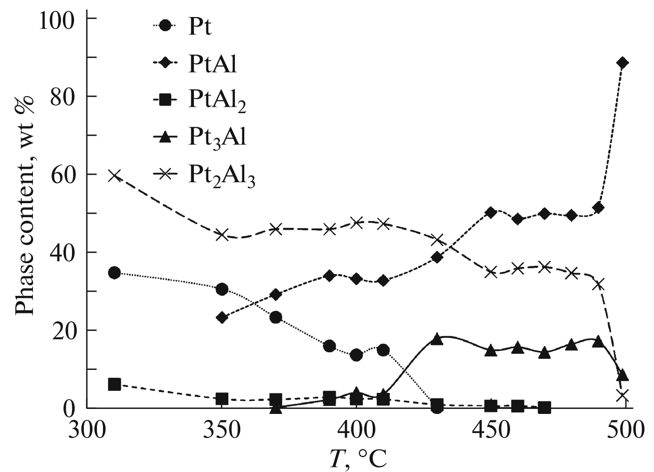

Fig. 3. Variation in the phase composition during the solid-state reaction in the Al/Pt films (wt %).

4. DISCUSSION

Based on the analysis of experimental results, we established that during the solid-state reaction in the Al/Pt bilayer thin films, the intermetallic compounds form in the following sequence (see Table 1):

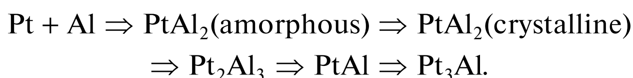

$$\mathrm{Pt + Al \Rightarrow PtAl_2(amorphous) \Rightarrow PtAl_2(crystalline) \Rightarrow Pt_2Al_3 \Rightarrow PtAl \Rightarrow Pt_3Al.}$$

It was shown that upon heating of the Al/Pt bilayer thin films the amorphous $PtAl_2$ phase starts forming when the temperature attains ~270°C. According to experimental studies [14, 15], during the solid-state reaction, the amorphous $PtAl_2$ phase forms first upon heating to a temperature of 200°C [15] and 300°C [14]; in works [16–19], the first crystalline phase forming after annealing at temperatures of 200–300°C is Pt_2Al_3. However, as was shown previously, the formation of $PtAl_2$ as the first phase does not agree with the theoretical calculations within the EHF [12] and Walser–Bene models [13], which predicted the primary formation of the Pt_5Al_{21} phase during the solid-state reaction at the Al/Pt interface. It should be noted that the EHF model [12], in contrast to the Walser–Bene one [13], takes into account the kinetic (effective concentration) and thermodynamic (heat formation) parameters, which allows it to predict not only the first phase, but also the total phase sequence. The sequence of phase formation in the solid-state reaction, according to the EHF model, is (the effective formation heat for each phase are given in parentheses) [12]

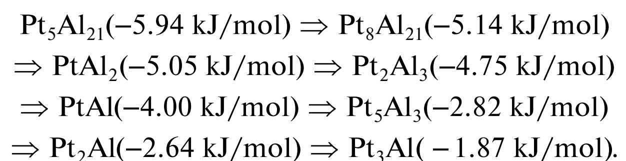

$$\mathrm{Pt_5Al_{21}(-5.94\ kJ/mol) \Rightarrow Pt_8Al_{21}(-5.14\ kJ/mol) \Rightarrow PtAl_2(-5.05\ kJ/mol) \Rightarrow Pt_2Al_3(-4.75\ kJ/mol) \Rightarrow PtAl(-4.00\ kJ/mol) \Rightarrow Pt_5Al_3(-2.82\ kJ/mol) \Rightarrow Pt_2Al(-2.64\ kJ/mol) \Rightarrow Pt_3Al(-1.87\ kJ/mol).}$$

The phases with the lowest effective formation heat should form before the rest ones.

The Pt_5Al_{21} and Pt_8Al_{21} phases have the lowest effective formation heat; however, as was shown in [12], the formation of these phases in thin films can be complicated by the existence of a nucleation barrier. This possibly causes the observed primary formation of the $PtAl_2$ phase in this work, which forms in the amorphous state. Upon further heating, the crystalline $PtAl_2$ and Pt_2Al_3 phases form almost simultaneously, which is explained by a small difference (~6%) between the effective formation heats (–5.05 and –4.75 kJ/mol, respectively) for these phases. This phenomenon was observed previously during the solid-state reaction in the Al/Au thin films [27]: the

Al_2Au_5 and $AlAu_2$ intermetallic compounds began growing almost simultaneously, which is also related to the minimum difference between the effective formation heats (−20.0 and −19.8 kJ/mol). The formation of the phase sequence $Pt_2Al_3 \Rightarrow PtAl \Rightarrow Pt_3Al$ observed in this study during the solid-state reaction corresponds to the phase sequence obtained in [18] and is explained by an increase in the effective formation heat of the phases Pt_2Al_3 (−4.75 kJ/mol) ⇒ PtAl (−4.00 kJ/mol) ⇒ Pt_3Al (1.87 kJ/mol).

The quantitative analysis of the phase content during the solid-state reaction showed that in the temperature range of 310–410°C, the content of the fcc platinum, Pt_2Al_3, and $PtAl_2$ phases decreases (Fig. 3). In addition, at this stage, the PtAl phase forms, but, due to the low absolute intensities of diffraction reflections of this phase, it can be unambiguously identified only after attaining a temperature of 350°C. An increase in the PtAl phase content in the temperature range of 310–410°C results from the reduction of the Pt_2Al_3, $PtAl_2$, and fcc platinum phase contents. Upon further heating, the increase in the PtAl phase content is mainly due to a decrease in the Pt_2Al_3 phase content in the temperature range of 410–500°C and the Pt_3Al phase content in the temperature range of 490–500°C. Further annealing at a temperature of 500°C for 30 min only led to a slight increase in the PtAl phase content.

Thus, in the temperature range of 350–500°C, the structural phase transformation of $Pt_2Al_3 \Rightarrow PtAl$ occurs and, in the temperature range of 490–500°C, $Pt_3Al + Pt_2Al_3 \Rightarrow PtAl$. The quantitative analysis of the phase content (Fig. 3) showed that in the temperature range of 410–430°C, the Pt_3Al phase content increases due to the structural phase transformation $Pt + PtAl \Rightarrow Pt_3Al$; simultaneously, the structural phase transformation $Pt_2Al_3 \Rightarrow PtAl$ occurs, which ensures an increase in the PtAl phase content.

Note that, in this study, we did not observe the formation of the following intermetallic compounds during the solid-state reaction: Pt_5Al_{21}, Pt_8Al_{21}, Pt_5Al_3, and Pt_2Al. The absence of Pt_5Al_{21} and Pt_8Al_{21} phases can be explained by the existence of nucleation barriers [12]. Concerning the Pt_5Al_3 and Pt_2Al phases, they should be formed, according to the EHF model, before Pt_3Al; meanwhile, the main diffraction reflections of all the three phases coincide. They can only be distinguished at their sufficient contents and a total set of reflections is observed in the electron diffraction pattern. In the temperature range from 390 to 429°C, the low-intensity diffraction reflections are observed, which can correspond to one of the Pt_3Al, Pt_5Al_3, or Pt_2Al phases and their mixtures. Only after attaining 430°C, one can unambiguously state that the film contains the Pt_3Al phase with a content of ~18 wt %.

5. CONCLUSIONS

The structural phase transformations were studied and a sequence of phases forming during the solid-state reaction in the Al/Pt bilayer thin films (the total thickness is up to 50 nm and the Al : Pt atomic ratio is ~1 : 1) was established. The investigations were carried out using in situ electron diffraction directly during the solid-state reaction initiated by heating in the transmission electron microscope column. It was shown that, at a temperature of ~270°C, the amorphous $PtAl_2$ phase forms during the reaction between the aluminum and platinum layers. Upon further heating, the $PtAl_2$, Pt_2Al_3, PtAl, and Pt_3Al crystalline phases sequentially form, which qualitatively agrees with the effective formation heat model. The contents of phases forming during the solid-state reaction were quantitatively analyzed. It was demonstrated that in the temperature range of 310–410°C, the PtAl phase forms due to a decrease in the contents of the fcc platinum, Pt_2Al_3, and $PtAl_2$ phases. In the temperature range of 410–430°C, due to the structural phase transformation $Pt + PtAl \Rightarrow Pt_3Al$, the Pt_3Al phase content grows; simultaneously, the structural phase transformation $Pt_2Al_3 \Rightarrow PtAl$ occurs, providing an increase in the PtAl phase content. Upon further heating, the PtAl phase content increases to ~90 wt % due to a decrease in the Pt_2Al_3 and Pt_3Al phase contents.

ACKNOWLEDGMENTS

This study was supported by the Russian Foundation for Basic Research, project no. 16-33-00475 mol_a.

REFERENCES

1. E. G. Colgan, Mater. Sci. Rep. **5**, 1 (1990).
2. *The Chemistry of Metal CVD*, Ed. by T. T. Kodas and M. J. Hampden-Smith (Wiley, New York, 2008).
3. A. S. Rogachev, Russ. Chem. Rev. **77**, 21 (2008).
4. D. P. Adams, Thin Solid Films **576**, 98 (2015).
5. B. K. Crone, I. H. Campbell, P. S. Davids, D. L. Smith, C. J. Neef, and J. P. Ferraris, J. Appl. Phys. **86**, 5767 (1999).
6. T. Biggs, M. B. Cortie, M. J. Witcomb, and L. A. Cornish, Platin. Met. Rev. **47**, 142 (2003).
7. R. Volkl, Y. Yamabe-Mitarai, C. Huang, and H. Harada, Met. Mater. Trans. A **36**, 2881 (2005).
8. W. S. Walston, in *Proceedings of the 10th International Symposium on Superalloys-2004*, Ed. be K. A. Green, T. M. Pollock, H. Harada, T. E. Howson, R. C. Reed, J. J. Schirra, and S. Walston (2004), p. 579.
9. Y. Noh and O. Song, Korean J. Met. Mater. **52**, 61 (2014).
10. K. W. Cho, T. W. Hong, S. Y. Kweon, and S. K. Choi, Korean J. Mater. Res. **14**, 688 (2004).
11. Y. S. Hwang, J. W. Lee, S. Y. Lee, B. J. Koo, D. J. Jung, Y. S. Chun, M. H. Lee, D. W. Shin, S. H. Shin, S. E. Lee, B. H. Kim, N. S. Kang, and K. N. Kim, Jpn. J. Appl. Phys. **37**, 1332 (1998).

12. R. Pretorius, T. K. Marais, and C. C. Theron, Mater. Sci. Rep. **10**, 1 (1993).
13. R. W. Bene, Appl. Phys. Lett. **41**, 529 (1982).
14. P. Gas, C. Bergman, G. Clugnet, P. Barna, A. Kovacs, and J. Labar, Def. Dif. Forum **194–199**, 807 (2001).
15. J. L. Labar, A. Kovacs, and P. B. Barna, J. Appl. Phys. **90**, 6545 (2001).
16. X. A. Zhao, E. Ma, H. Y. Yang, and M. A. Nicolet, Thin Solid Films **153**, 379 (1987).
17. E. Ma and M. A. Nicolet, Phys. Status Solidi A **110**, 509 (1988).
18. E. G. Colgan, J. Appl. Phys. **62**, 1224 (1987).
19. M. Nastasi, L. S. Hung, and J. W. Mayer, Appl. Phys. Lett. **43**, 831 (1983).
20. S. P. Murarka, I. A. Blech, and H. J. Levinstein, J. Appl. Phys. **47**, 5175 (1976).
21. ADVENT Research Materials Ltd., Oxford, U.K. www.advent-rm.com.
22. S. M. Zharkov, E. T. Moiseenko, R. R. Altunin, N. S. Nikolaeva, V. S. Zhigalov, and V. G. Myagkov, JETP Lett. **99**, 405 (2014).
23. E. T. Moiseenko, R. R. Altunin, and S. M. Zharkov, Phys. Solid State **59**, 1233 (2017).
24. S. M. Zharkov, R. R. Altunin, E. T. Moiseenko, G. M. Zeer, S. N. Varnakov, and S. G. Ovchinnikov, Solid State Phenom. **215**, 144 (2014).
25. J. L. Labar, Microscopy Microanal. **15**, 20 (2009).
26. H. Putz, J. C. Schön, and M. Jansen, J. Appl. Crystallogr. **32**, 864 (1999).
27. G. Majni, C. Nobili, G. Ottaviani, and M. Costato, J. Appl. Phys. **52**, 4047 (1981).

Translated by E. Bondareva